Characterization of ultrafine particles and the occurrence of new particle formation events in an urban and coastal site of the Mediterranean area

Adelaide Dinoi[1], Daniel Gulli[2], Kay Weinhold[3], Ivano Ammoscato[2], Claudia R. Calidonna[2], Alfred Wiedensohler[3], Daniele Contini[1]

[1]Institute of Atmospheric Sciences and Climate, ISAC-CNR, S. P. Lecce-Monteroni km 1.2, 73100 Lecce, Italy
[2]Institute of Atmospheric Sciences and Climate, ISAC-CNR, Zona Industriale, I-88046 Lamezia Terme (CZ), Italy
[3]Leibniz Institute for Tropospheric Research, 04318, Leipzig, Germany

Correspondence to: Adelaide Dinoi (a.dinoi@isac.cnr.it)

Abstract. In this work, new particle formation events (NPF) occurringed at two locations in Southern Italy, the urban background site of Lecce (ECO station) and the coastal site of Lamezia Terme (LMT station), are identified and analysed. The study aims to compare the properties of NPF events at the two sites located 225 km away from each other and characterized by marked differences in terms of emission sources and local weather dynamics. Continuous measurements of particle number size distributions, in the size range from 10 nm to 800 nm, were performed at both sites by a Mobility Particle Size Spectrometer (MPSS). The occurrence of NPF events, observed throughout the study period that lasted five years, produced different results in terms of frequency of occurrence, 25 % of the days at ECO and 9 % at LMT. NPF events showed seasonal patterns, higher frequency during spring and summer at the urban background site, while at the coastal site during the autumn-winter period. Some of these events happened simultaneously at both sites, indicating the occurrence of the nucleation process on a large spatial scale. Cluster analysis of 72 h back-trajectories showed that during the NPF events the two stations were influenced by similar air masses, most of which originated from the North-Western directions. Local meteorological conditions characterized by high pressure, with a prevalence of clear skies, low levels of relative humidity (RH < 52 %), and moderate winds (3-4 m s^{-1}) dominated the NPF events at both sites. Notable differences were observed in SO_2 and $PM_{2.5}$ concentrations and H_2SO_4 proxy levels, resulting in ~65 %, ~80 %, and 50% lower at LMT compared to ECO, respectively. It is likely that the lower level of that recognized as one of the main gas precursors involved in the nucleation process, can be responsible for the smaller NPF frequency of occurrence (~60 % less than ECO) observed in LMT.

1 Introduction

The formation of new particles (NPF), by nucleation of gas-phase species and consecutive growth, is an important atmospheric process that contributes to producing high levels of ultrafine particles (UFP, diameter < 100 nm). Together with primary

emission sources, natural and anthropogenic, the nucleation represents a significant source of secondary ultrafine aerosol particles and cloud condensation nuclei (Merikanto et al., 2009; Yu et al., 2020), accounting for about 50 % of the production of particle number concentration on a global scale. Due to their size, high number concentration, and chemical composition, these particles have profound implications on the environment, climate, and public health (Zhang et al., 2015; Sartelet et al., 2022) which emphasize their relevance.

The formation of new particles was observed and investigated in various geographic locations, under different atmospheric and environmental conditions, from which common characteristics and different peculiarities emerged (Baalbaki et al., 2021; Jokinen et al., 2022; Yadav et al., 2021; Franco et al., 2022).

The new particle formation can occur on a local scale, typically characterized by an intense burst (strong intensity) of secondary particle formation of short duration and without subsequent growth (Dai et al., 2017), usually related to local anthropogenic emissions (Hussein et al., 2014), or else it can manifest as a part of an event which takes place on a large spatial scale (regional event). In this case, the nucleation process can originate from several hundred kilometers away from the measurement site (Dall'Osto et al., 2013; Németh and Salma 2014; Zhu et al., 2014), and the newly-formed particles can be contemporary observed in multi-location measurements.

~~Such regional events were documented in the literature by various authors, i.e. in the work by Nemeth et al. (2018) 12 NPF events were observed simultaneously at three European cities located within a distance of 450 km, Budapest, Vienna, and Prague; during two years measurement campaign, Kalkavouras et al. (2020) observed 35 simultaneous NPF events that occurred at the urban site of Athens and the regional background site of Finokalia, located 340 km away. Concomitant NPF events were also detected in the spring of 2002 in the city of Leipzig and three other locations situated 10-50 km away each other (Wehner et al., 2007), as well as regional NPF events were recorded in two sites of Finland, Hyytiälä and Värriö, that situated within a distance of 220 km (Hussein et al., 2009).~~ It was noted that most NPF events occurred in analogous conditions, under the influence of air masses with the same origin and enriched with sulfur-rich precursors (Kalkavouras et al., 2020), and exhibiting similar dynamic characteristics. NPF events were usually detected in ground-based measurement stations, but a number of observations were also performed at high altitudes, on mountain tops (Rose et al., 2015; Bianchi et al., 2016), by balloons and through aircraft (Schroder and Strom, 1997; Mirme et al., 2010) leading to hypothesize that the nucleation process can be triggered within the atmospheric column, at different heights (Boulon et al., 2011; Minguillón et al., 2015; Querol et al., 2017), both throughout the boundary layer and in the free troposphere. At upper atmospheric levels, nucleation would be facilitated by the higher dilution of the pollutants (low condensation sink) and by enhanced photochemical conditions. Once nucleated, the particles can be transported over long distances by the circulation of air masses. Where and at which altitude the mechanism is triggered is still unclear (Boulon et al., 2011), but in this process atmospheric dynamics could play a crucial role in the mixing of precursor gases and/or pre-existing particles, influencing their occurrence and spatial distribution (Wehner et al., 2015).

To date, the variability of the conditions and the complexity of the phenomenon make our knowledge of this process still fragmentary in many aspects. While it is well known that solar intensity, low relative humidity, and the availability of high

levels of aerosol nucleation precursors (sulfur dioxide, ammonia, amines, VOCs) are common features in the NPF (Wu et al., 2021), the chemical/physical mechanisms involved in the process remain uncertain and further insights are required.

In this paper, we summarize the results of a long-term study on the new particle formation events carried out at two sites in southern Italy, Lecce (ECO station) and Lamezia Terme (LMT station). To the best of our knowledge, this work represents one of the few long-term studies on NPF events conducted in the Mediterranean area and the first one conducted in Italy. Based on a 5-yr period, simultaneous measurements of aerosol particle number size distribution were analysed with the aim to characterize, investigate, and compare the relationship of NPF events with meteorological and pollution data at a coastal and an urban background site. To support interpretations, simultaneous measurements of SO_2 and $PM_{2.5}$ ambient concentrations were carried out at both ground monitoring stations. The role of air mass and local meteorological factors were also investigated.

~~**2 Methodology**~~

~~**2.1 Study area**~~

2 Measurements and methods

2.1 Measurement sites and instrumentation

Measurements of particle number size distribution (PNSD) were made from January 2015 to December 2019 at two sites of southern Italy, Lamezia Terme Observatory (LMT, 38.88° N, 16.23° E, 6 m a.m.s.l.,) in Calabria region, and Lecce Observatory (ECO, 40.20° N, 18.07° E, 50 m a.m.s.l.) in Puglia region. The locations of the measuring sites are depicted in Fig. 1. ECO and LMT, both regional stations of GAW/ACTRIS networks, are representative of urban backgrounds and suburban/coastal sites, respectively. ECO observatory is located inside the University Campus (Dinoi et al., 2020), about 5 km southwest of the municipality of Lecce, while the LMT observatory is located about 17 km from the urban city and about 600 m inland from the Tyrrhenian coastline, at an elevation of 6 m above sea level (a.s.l.). The two sites are about 225 km as the crow flies. The municipalities cover areas of 238 km^2 (Lecce) and 160 km^2 (Lamezia) with populations of 95,000 and 70,452 inhabitants respectively. Their climate is Mediterranean, albeit characterized by different local meteorological ~~dynamics~~ conditions. Being on the coast, the local weather of LMT is influenced by a system of "land-see" breezes that guarantees a temperate climate and continuous ventilation throughout the year that favors an effective dilution of air pollutants. Different emission sources (more details from Cristofanelli et al., 2018; Calidonna et al., 2020; Dinoi et al., 2021b) affect the two sites. The main aerosol sources in the ECO observatory are the emissions of vehicular traffic and biomass combustions, which are added to natural and anthropogenic long-range contributions (Donateo et al., 2018; Conte et al., 2020). The site is characterized by frequent conditions of clear skies during the whole year, with mild autumn-winter seasons and warm spring-summer. ~~Due to its location, away from the urban agglomeration, T~~the LMT observatory is located far from the urban agglomeration and therefore is not directly ~~is weakly~~ affected by the ~~main~~ emission ~~sources~~ deriving from the main anthropogenic activities.

~~**2.2 Instruments**~~

Aerosol PNSD from 10 to 800 nm, with a time resolution of 5 minutes, were collected using a TROPOS-type custom-built MPSS (Mobility Particle Size Spectrometer), designed and manufactured according to EUSAAR/ACTRIS recommendations (Wiedensohler et al., 2012). ~~The instruments used are the same at the two stations as well as the calibration and data quality control procedures used. The two MPSS consist of a bipolar diffusion charger (Ni-63), a differential mobility analyzer (Vienna-type DMA, length 28 cm), and a condensation particle counter (CPC, model: TSI 3772, TSI Inc., Rome, Italy).~~ It is a closed-loop system, with a 5:1 ratio between the sheath and aerosol flow, where the sample air is drawn into the instrument at a flow rate of 1 l/min, while the sample humidity is regulated below 40 % by a Nafion dryer. The two MPSS consist of a bipolar diffusion charger (Ni-63), a differential mobility analyzer (Vienna-type DMA, length 28 cm), and a condensation particle counter (CPC, model: TSI 3772, TSI Inc., ~~Rome, Italy~~ USA). The instruments used are the same at the two stations as well as the calibration procedures, carried out periodically, and data quality control. The quality of measurements of both instruments was routinely checked and all data were corrected for particle losses by diffusion and ~~negative~~ multiple charged particles according to the recommendations of Wiedensohler et al., (2012). Concentrations of sulphur dioxide (SO_2) were measured using Thermo Instruments analyzers, TEI 43i, and $PM_{2.5}$ mass concentrations using low-volume samplers with a β-ray attenuation method (SWAM 5a Dual Channel Monitor (FAI Instruments). Local meteorological parameters, air temperature (T), relative humidity (RH), precipitation (Rain), wind speed (WS), and wind direction (WD) were monitored by automatic weather stations (Vaisala WXT 520), located in the two observatories while solar radiation (solar flux) was collected by CNR 4 net radiometers (Kipp&Zonen). Air mass back trajectories were calculated using the HYSPLIT 4 model developed by NOAA/ARL, a single particle Lagrangian trajectory dispersion model (Stohl 1998).

~~**2.3 Evaluation of NPF events**~~

2.2 Data analysis

Classification of NPF events was performed by visual inspection of daily contour plots (Dal Maso et al., 2005). Examining the time evolution of the particle number size distribution, three main classes were detected: NPF events, non-events, and undefined events. NPF events contain cases where a significant increase in the number concentrations of ultrafine particles and growth toward larger diameters was observed for at least 3 - 4 h continuously, displaying the shape of a “banana”. “Non-events” are the days without new particle formation, while “undefined events” group ambiguous cases, with unclear formation and growth, or the occurrence of newly formed particles below 20 nm without the next phase of growth.

Particle growth rate (GR) was calculated from time evolution of the mean geometric diameter D_p in the size range of 10-20 nm, using Eq. (1) (Kulmala et al., 2012):

$$GR(nm\ h^{-1}) = (D_{p2} - D_{p1})/(t_2 - t_1) \quad (1)$$

with Dp_1 and Dp_2 the geometric diameter at the start time t_1 and end time t_2 of the growth event. Using the maximum concentration method (Lehtinen et al., 2003), we identified the time when the concentration is at the maximum in each size bin of the measured particle number size distributions. The growth rates were obtained as the slope of the linear fit of the times with the corresponding geometric mean diameters of the size bin particles.

The condensation sink, CS (s^{-1}), quantifies how rapidly a condensable gaseous compound condenses on available aerosol particles (Kerminen et al., 2018), and then it depends on the effective surface area of pre-existing particles. CS was calculated using the methods available in the literature (Dal Maso et al., 2005, and references therein) considering sulphuric acid (H_2SO_4) as the condensable species:

$$CS = 2\pi D \sum_{D'_p} \beta_m(D'_{pi}) D'_{pi}\, N_i \quad (2)$$

where D is the diffusion coefficient for H_2SO_4, N_i is the particle number concentration with diameter D'_{pi} of the size bin i, and β_m is the transition correction factor (Fuchs et al., 1971).

The formation rate, J ($cm^{-3}s^{-1}$), defined as the flux of changes in particle number concentration within the nucleation mode size range (10–20 nm), was estimated by (Dal Maso et al., 2005; Kulmala et al., 2012):

$$J = \frac{dN_{nuc}}{dt} + CoagS_{nuc} * N_{nuc} + \frac{GR}{\Delta dp} N_{nuc} \quad (3)$$

with (dN_{nuc}/dt) the temporal change rate of nucleation mode particle number concentration, ($CoagS_{nuc} \cdot N_{nuc}$) the loss caused by collision process and by growth process ($GR \cdot N_{nuc}/\Delta dp$).

Sulfuric acid (H_2SO_4) is considered a key precursor for new particle formation, therefore its concentrations were derived by calculating the H_2SO_4 proxy, without scaling factor, using the method presented by Petäjä et al. (2009):

$$[H_2SO_4]\alpha \frac{SO_2 \times SRad}{CS} \quad (4)$$

where SO_2 is the sulphur dioxide concentration, $SRad$ is the solar radiation flux, and CS the condensation sink.

3 Results and discussions

3.1 Classification of NPF events

The relative frequency of the different classes, events, non-events, and undefined events was calculated for both sites and summarized in Table 1. Over five years of measurements, we had a data coverage of ~78 %, where ~~T~~the available measurement days were 1423 at ECO and 1440 at LMT ~~with a data coverage of ~78 %~~. The missing days were due to technical/maintenance problems of the MPSS or measurement failures and mainly concerned the months of February/March for LMT, and January for ECO. ~~Of these,~~ Among the available data, 25 % and 9 % of days were identified as NPF events while 4% and 3% as undefined events at ECO and LMT, respectively. We found that the percentage frequency of NPF events is higher in ECO than in LMT, with differences in the monthly and seasonal occurrence of the events (Fig. 2). At the ECO site the highest frequencies of NPF events were observed in March and September (~30 %) and the lowest in November and December (12 % -16 %), ~~confirming what was already observed in~~ showing similar results to those found in a shorter measurement period

presented by Dinoi et al. (2021a). At LMT, March (19 %) and October (16 %) showed the highest frequencies while July and August were the lowest ones (2 - 3 %). Consequently, this is reflected in a different seasonality of events, more frequent in spring and summer in ECO, and in autumn and winter in LMT. Of all events detected during the study period, 50 were observed simultaneously at both sites. Due to the complementary frequency, most of them occurred in the colder months, ~ 23 % in winter and spring, 14 % in summer, and 39 % in autumn. The annual frequencies of NPF (9% and 25 %) are in good agreement with frequencies (10 % - 36 %) found in other studies, based on long-term measurements, carried out in the Mediterranean area (Kopanakis et al., 2013; Kalivitis et al., 2019; Hussein et al., 2020; Kalkavouras et al., 2020; Baalbaki et al., 2021). The seasonal variability observed in the ECO site was also similar to that found in several other locations (in Europe and around the world) and can be ascribed to the higher emissions of biogenic aerosol precursor compounds and photochemical processes promoted by the higher temperature during the warmer months (Asmi et al., 2016). However, the opposite trend displayed by the LMT site is not a novelty since it has also been observed, albeit less frequently, in other southern Europe sites. In Spain and Greece, for example, Bousiotis et al. (2021) found the occurrence of a larger number of NPF events just during winter and that might be linked to the specific meteorological conditions of the study area.

~~The temporal evolution of the events was very similar between the two sites, the start times were in the morning between 9:00 – 12:00 with a median duration of hours, similar to what was observed by Dinoi et al. (2021a).~~

~~Typically, the particle growth rates were high during the first few hours of nucleation and then decreased to a few nanometers per hour within 3-4 hours after nucleation. The growth rate of particles varied between 3nm h^{-1} and 14 nm h^{-1} with a mean and standard deviation of 7.5 ± 3.3 nm h^{-1} in ECO, and between 2.5 nm h^{-1} and 10 nm h^{-1} with a mean and standard deviation of 6.1 ± 2.3 nm h^{-1} in LMT. In general, lower GR is observed in a clean environment and vice versa, but because many factors are involved in the NPF process, this behavior is not always observed.~~

3.2 Atmospheric particle number concentration (PNC)

A statistical overview of the ~~emission levels~~ concentrations and contributions of three diameter modes particles, nucleation (N_{nuc}=N_{10-20}), Aitken (N_{Aitk}=N_{20-100}), and accumulation (N_{acc}=$N_{100-800}$), to total particle number concentration (N_{tot}=N_{10-800}) was made. ~~For each observatory, arithmetic means ± 1 standard deviation, medians, and percentiles (25th 75th) of PNC were calculated from the daily data and~~ As summarized in Table 2 (arithmetic means ± 1 standard deviation, medians, and percentiles (25th-75th)), the mean value of total PNC was (4.4 ± 2.2) x 10^3 cm^{-3} at LMT and (7.8 ± 3.4) x 10^3 cm^{-3} at ECO. Although significantly higher concentrations (about 40 %) were found at the urban background site compared to the coastal site, the contribution of each particle fraction to total particle number concentration was very similar, 24 %, 49 %, and 27 % in LMT and 20 %, 52 % and 28 % in ECO, for nucleation, Aitken, and accumulation mode particles, respectively. In both cases, Aitken mode particles represented the largest fraction of particle number concentrations.

The levels measured at two sites are within the range reported for similar locations observed in other European sites (Putaud et al., 2010; Asmi et al., 2011; Kalivitis et al., 2019; Casquero-Vera et al., 2020; Kalkavouras et al., 2020). The monthly

variability of PNC, averaged over the whole study period, is shown in Fig. 3. In ECO and LMT the highest monthly average concentrations of Aitken mode particles were observed during winter (~5.6 x 10^3 cm^{-3} and ~2.7 x 10^3 cm^{-3}), approximately 45 % in ECO and 35 % in LMT higher than in summer (~3.2 x 10^3 cm^{-3} and ~1.7 x 10^3 cm^{-3}). In ECO accumulation mode particles ranged from~1.7 x 10^3 cm^{-3} in spring to ~3.1 x 10^3 cm^{-3} in winter, while in LMT from ~9.8 x 10^2 cm^{-3} in autumn to ~1.4 x 10^3 cm^{-3} in summer. The increase in N_{acc} concentration during the summer can be ascribed to the dry conditions that characterize the Mediterranean summers (Pikridas et al., 2018). Nucleation mode particles displayed a similar seasonal pattern to Aitken mode particles in LMT (from ~8.0 x 10^2 cm^{-3} in summer to~1.4 x 10^3 cm^{-3} in winter), while in ECO values slightly higher were observed during spring/summer, ~1.9 x 10^3 cm^{-3}, than in winter ~1.3 x 10^3 cm^{-3}. The higher concentrations recorded during cold months are generally associated with enhanced anthropogenic emissions from fossil fuel combustion and biomass burning, due to residential heating, and unfavourable meteorological conditions for pollution dispersion.~~, such as frequent occurrences of stagnant weather and temperature inversion.~~

A clear diurnal pattern in each mode particle number concentration was observed in every season. Fig. 4 shows the trend of each mode fraction considering separately the days of NPF events (E, solid line) and the days of non-events (NE, dashed line). The timing of measurements is expressed in solar time (UTC + 1). Nucleation, Aitken, and accumulation mode particles have very similar behavior during non-events and, except for the different concentrations, both sites show a pronounced diurnal cycle with a morning and evening peak. The two peaks are shifted by one hour between spring-summer and autumn-winter because of daylight savings time and are mainly linked to vehicular emissions, most intense during the morning and evening rush hour. ~~The diurnal variation of concentrations at the ground level is governed not only by the emission sources but also by the dynamics (height and stability) of the PBL. Stagnant conditions and low PBL during early mornings and late evening exacerbate morning/evening rush hour pollution and help to build up pollution levels associated with primary emissions, mainly from traffic (Backman et al., 2012). At noon, the height of the PBL increases favouring the mixing of pollutants throughout the PBL and limiting their accumulation at ground level.~~ In addition, the evening peaks of Aitken and accumulation mode particles in winter and autumn can be linked to domestic heating emissions, mainly biomass burning, considered an important source of ultrafine particles in urban sites. In cold months these particles tend to accumulate during the night due to the reduced boundary layer compared to the daytime layer. These peaks are also present in LMT but are less intense due to the greater distance of the site from the urban centre. ~~A different situation was observed for nucleation mode particles, wherein~~ Regarding event days, in both sites, together with the two peaks of rush hours, nucleation mode particles present further picks ~~are present~~ around noon, more marked in summer, spring, and winter in ECO, and spring, summer, and autumn in LMT. Less pronounced are instead those in winter and autumn in LMT and ECO respectively.

~~The difference in number concentration attributed to nucleation processes is notable by which the concentrations of particles in nucleation mode are strongly influenced.~~ Similar observations have been reported in Cusack et al. (2013), Kalivitis et al. (2019), Kalkavouras et al. 2020, Dinoi et al. (2020, 2021a), for the western Mediterranean sites where the diurnal variation in nucleation mode particles presents a clear maximum at noon under both polluted and clean conditions. The contribution of the NPF process to the number concentration is also observed in the Aitken mode particles, more noticeable in the LMT site with

30 % in autumn-winter and 41 % in spring-summer, and with 21 % only in spring-summer in the ECO site. In Table 3 is reported mean values ± 1 standard deviation of nucleation, Aitken and accumulation of PNC (cm^{-3}) related to event days (E) and non-event days (NE) for each season (winter W, spring Sp, summer S, and autumn A) in both sites. Nucleation mode particles show an increase of 52 %, 65 %, 61 %, and 49 % in winter, spring, summer, and autumn in LMT, and of 47 %, 52 %, 55 %, and 39 % in ECO. These results highlight that the formation of new particles contributes to the overall particle population more in the warm months and more significantly in the coastal site than in the urban background site, probably because the urban site is also affected by local emission of ultrafine particles that tend to suppress the NPF process.

No contribution is observed in the concentration of accumulation mode particles where especially in the first half of the day, the concentrations were higher on non-event than event days, especially at the ECO site. This could explain the different frequency of events that characterized the two sites in these seasons, assuming that the NPF events were favored on those days with lower particle number concentrations (Salma et al., 2017).

The relative increase in particle number concentration due to the NPF process was also quantified with the nucleation strength factor (NFS) proposed by Salma et al. (2016, 2017, 2019). It measures the effects of nucleation events on ultrafine particles at a site considering two factors, NSF_{NUC} that provides a measure of the concentration increment on nucleation days exclusively caused by NPF, and NSF_{GEN} that gives a measure of the overall contribution of NPF over a longer time span. In this work we considered only NSF_{NUC}, calculated following Eq. (5):

$$NFS_{NUC} = \frac{(N10-100)/(N100-800)_E}{(N10-100)/(N100-800)_{NE}} \quad (5)$$

with N10−100 / N100−800 the concentration ratios for nucleation days at the numerator and the N10−100 / N100−800 concentration ratios for not nucleation days at the denominator. Depending on the value, NFS_{NUC} <1.0, 1.0 < NFS_{NUC} <2.0, or NFS_{NUC} >2.0, the nucleation process can be considered negligible, comparable to the other sources or the main contributor. In LMT the mean values of NFS_{NUC} were 2.0, 2.1, 2.3, and 1.9 while in ECO 1.7, 1.6, 1.9, and 1.9 in winter, spring, summer, and autumn, respectively. From the coastal to urban background site, we found a decrease in the contribution of NPF events to particle number, similar to what was observed by Salma et al. (2017) between the near city background (2.3) and the city center (1.6) of Budapest over 5 years. In the study of Bousiotis et al. (2021), on 13 sites from five countries in Europe it was found that for almost all rural background sites NFS_{NUC} was greater than 2, and reached 4 in a very clean site of Finland. Nemet et al. (2018) found lower values of NFS_{NUC}, 1.58, 1.54, and 2.01, in the cities of Budapest, Vienna and Prague, respectively, while in Granada urban site NFS_{NUC} was 1.05 (Casquero-Vera et al., 2021). The decrease in the contribution of NPF events to particle number, moving from a less polluted to a more polluted site, may be related to the higher contribution to particle number concentrations of other sources, i.e. traffic and heating, and the associated increased condensation sink. These results point out that the particles produced by the NFS_{NUC} process can become the dominant sources in a clean environment compared to more polluted areas.

3.3 Factors associated with NPF events

The growth rate (GR) and the particle formation rate (J) were analyzed to investigate the dynamic properties of NPF events. At the ECO site the growth rate values ranged from 3nm h^{-1} to 14 nm h^{-1} (average 7.5 ± 3.3 nm h^{-1}) and J from 0.6 to 8.6 cm^{-3} s^{-1} (average 3.3 ± 3.1 cm^{-3} s^{-1}); while at LMT the GR varied from 2.5 to 10 nm h^{-1} (average 6.1 ± 2.3 nm h^{-1}) and the J from 0.3 to 6.2 cm^{-3} s^{-1} (average 2.4 ± 1.8 cm^{-3} s^{-1}). The values of both parameters are comparable with what was reported for NPF events in other urban and coastal sites (Hussein et al., 2020, Kalivitis et al. 2019; Salma et al.(2019), Kalkavouras et al., 2020; Nieminen et al. 2018). In particular, similarities were found with some Mediterranean sites such as the coastal station of Finokalia GR~ 5 nmh^{-1}, J~ 0.9 cm^{-3} s^{-1} (Pikridas et al., 2012), the coastal/rural/suburban station of Akrotiri, GR~ 6 nmh^{-1}, J~13 cm^{-3} s^{-1} (Kopanakis et al., 2013) and the Cyprus Island, GR~ 2.8–5 nmh^{-1}, J~ 5–11.4 cm^{-3} s^{-1} (Debevec et al., 2018). The mean values of GR and J turned out to be higher at the ECO site than at the LMT site, and they showed a clear seasonal pattern with higher values during warm months, not observed at LMT where both parameters did not show distinctive features. As reported by Nieminen et al. (2018), the production rate of nucleation particles is generally higher in urban sites than in remote/clean ones because of the greater availability of precursors deriving from greater anthropogenic activity. In particular, the higher values of GR and J in warm months can be attributed to the intensification of the photochemical activity and abundance of SO_2 which acts as a precursor of sulfuric acid. ~~Since there are many factors involved in the process, direct measurements of $PM_{2.5}$ and SO_2 concentrations, and meteorological variables, performed at both sites, including the condensation sink were compared. The CS was estimated from measurements of the particle number size distribution between 10 and 800 nm, more details on the CS calculation are in the literature (Dal Maso et al., 2005; Kulmala et al., 2004 and references therein).~~ In this perspective, we investigated the effects of $PM_{2.5}$, CS, and SO_2 concentrations on the occurrence of NPF at both sites ~~There~~ where visible differences in pollution load (Fig. 5) were found ~~at the two sites~~. The average $PM_{2.5}$ and SO_2 concentrations during event days were 2.5±1.5 μg m^{-3} (ranging from 2.0 to 3.8 μg m^{-3}) and 0.4±0.3 ppb (from 0.2 to 0.6 ppb) for LMT, while they were 12.0±6.0 μg m^{-3} (from 9.5 to 15.3 μg m^{-3}) and 1.1±0.4 ppb (from 0.8 to 1.3 ppb) for ECO. These values were compared with mean values of $PM_{2.5}$ and SO_2 measured on non-event days, 6.1±2.5 μg $m^{-3}$and 0.2±0.2 ppb in LMT, 15.5±8.0 μg m^{-3} and 0.9±0.4 ppb in ECO. In both sites statistically significant differences (p-value <0.05 level, by Wilcoxon-Mann-Whitney test) emerged, highlighting the different role they may have played in the new particle formation. CS, estimated from measurements of the particle number size distribution between 10 and 800 nm, was (0.7 ± 0.3) x 10^{-2} s^{-1} (0.005 - 0.009 s^{-1}) for LMT and (1.0 ± 0.6) x 10^{-2} s^{-1} (0.008 - 0.01 s^{-1}) for ECO, within the range of coastal and urban environments (Salma et al., 2016; Kalivitis et al., 2019; Baalbaki et al., 2021). In this case, the comparison with values measured during non-event days, (0.7± 0.4) x 10^{-2} s^{-1} in LMT and (1.3 ±0.5) x 10^{-2} s^{-1} in ECO showed no noteworthy differences. The two sites displayed evident differences in both concentrations, with SO_2 ~65 %, $PM_{2.5}$ ~80 %, and CS ~30 % lower in LMT than ECO. This underlines how the two areas are affected in different ways by anthropogenic contributions, and the lower levels of SO_2 could be responsible for the reduced NPF frequency (~65 % less than ECO) observed in LMT. In

general, particulate matter concentration has a direct effect on the condensation sink that quantifies how rapidly a condensable gaseous compound condenses on available aerosol particles (Kerminen et al., 2018). As known, new particle formation is ~~discouraged~~ not favoured by the high concentration of pre-existing particles because they increase condensation sink (CS) for vapours. ~~Therefore, it was surprising to discover the low frequency of nucleation events occurred at LMT that being a cleaner site compared to Lecce we would have expected the opposite result (Dinoi et al., 2017; Dinoi et al., 2021b).~~ Therefore, lower CS would favour nucleation proportionally to the amount of condensable vapours available (Saha et al., 2018). Sulphuric acid is identified as one of the key components directly connected to NPF process (Sipila et al., 2010). Because no direct measurements of it were done in this study, we investigate its role, considering the proxy of sulphuric acid (Eq.4), without scaling factor (Petaja et al. 2009). The proxy only allows us to estimate the order of the average concentration levels of H_2SO_4 and although the results obtained are subject to uncertainties, they can still provide indications of trends (Salma et al., 2019). The average monthly values of H_2SO_4 proxy showed substantial differences between the two sites on event days (Fig 5d), 40 $x10^3$ ppbWm^{-2}s (ranging from 18 $x10^3$ to 61 $x10^3$ ppbWm^{-2}s) at ECO and 20$x10^3$ ppbWm^{-2}s (from 11 $x10^3$ to 38 $x10^3$ ppbWm^{-2}s) at LMT. These values are about 35% higher than non-events days in both cases. The proxy values of H_2SO_4 are larger in warm months and are substantially higher, by a factor of 2, in the urban background than in the coastal site, mainly due to the values of CS and SO_2. These last results are in accordance with GR and J values obtained for the two sites, where the low J and GR values at LMT could be associated with the low concentrations of H_2SO_4 (or other precursors). The conditions for the occurrence of NPF events are mainly driven by the ratio of the source and sink terms for the condensing vapors, therefore a greater availability of this gas precursor could have favored the occurrence of NPF events at ECO, although the higher values of CS, as well as the lower levels could have limited its development at LMT. ~~Lower CS would favour nucleation proportionally to the amount of condensable vapours available (Saha et al., 2018). In this case, LMT exhibits low levels of both factors, SO_2 and CS (so as $PM_{2.5}$) which would explain the observed results. The proportionality between the lower frequency of nucleation events and the lower SO_2 concentrations observed between the two sites was already noted in other works. Saha et al. (2018) highlight how, in the urban background of Pittsburgh, the large reduction of SO_2 concentrations (~90 %) over 15 years resulted in the reduction of nucleation frequency of ~70 %, as well as Kyrö et al. (2013) observed that the decrease in new particle formation days is the result of the reduction of sulphur emissions originating from Kola Peninsula (Russia). Hamed et al. (2010) observed at the atmospheric research station of Melpitz (Germany) that decreasing SO_2 concentrations by an average of 65 % led to a 45 % decrease in the frequency of NPF events, while Gaydos et al. (2005) simulated that a substantial reduction in SO_2 (more than 40 %) would reduce proportionally nucleation with different effects depending on the season.~~

3.4 Meteorological conditions and air masses associated with NPF events

The comparison of the main meteorological parameters was carried out to better characterize the occurred NPF also in terms of the local climate of the two study areas. The monthly average values of solar flux, relative humidity, and wind speed were calculated starting from the daily averages. All NPF events happened in comparable weather conditions featured by high pressure, with a prevalence of clear skies, typical of the Mediterranean climate. ~~First of all, we considered solar flux, one of the main factors involved in the nucleation process (Fig. 6a).~~ Monthly mean values showed an intense solar flux both in LMT (from 260 to 512 W m^{-2}) and in ECO (from 230 to 510 W m^{-2}) during events (columns). These values were very similar to those measured during non-event periods except at the LMT site where higher mean values are observed in the colder months, differences which however are not statistically significant. During event days, the RH was comparable at the two sites: 52 ± 4 % in LMT and 50 ± 7 % in ECO, and it was about 25 % lower than that on non-event days (Fig. 6b). This result is not a novelty because lower RH is usually observed during NPF events in both clean and polluted environments (Kerminen et al., 2018). On average, monthly wind speeds were higher during events in both sites, 4 ± 1 m s^{-1} for LMT (from 2.9 to 5.4 m s^{-1}) and 3 ± 1 m s^{-1} for ECO (from 2.6 to 4.3 m s^{-1}), respectively about 10% and 40% higher than the wind speed observed on non-event days (Fig. 6c). The difference is statistically significant only for ECO (p-value <0.05). Regarding the wind directions (Fig. 7) in ECO the dominating wind direction was mainly from N–NNW, with a frequency of occurrence of 75 %, while inLMT from E-NE and W-NW, with a frequency of occurrence of 30 % and 55 %, respectively, corresponding to a land-sea breeze system. The two prevalent wind directions together with the higher wind speed (both on events and on non-event days) are typical of a coastal area where generally, thanks to the circulation of the sea-land breeze, wind speed is approximately 20 % greater than in the innermost (inland) sites and almost constant during the whole year (Jensen et al., 2017). The breezes influence the diffusion of atmospheric pollutants and their dilution, thus explaining the low and almost constant (lack of seasonality) levels of PM measured at LMT.

~~3.5 The role of air masses associated with NPF events~~

~~As well known,~~ Also, the origin and pathways of air masses can contribute significantly to the occurrence of NPF processes (Wonaschutz et al., 2015). Depending on their advection pattern, air masses can be affected by emission sources and chemical/physical processes able to influence the properties of the pollutants during transportation. With this aim, the role of air masses was investigated through the analysis of the back trajectories of all days identified as NPF events. 72 h back trajectories were computed each day at 08:00 UTC, with 6 h resolution, at the 500 m height arrival above ground level (AGL), using the HYSPLIT 4, single-particle lagrangian trajectory dispersion Model, developed by NOAA/ARL (Draxler and Hess, 1998). We considered only the back trajectories at an altitude of 500 m because they can be better correlated with ground-based measurements and, therefore, more representative of the atmospheric boundary layer in which air pollutants are well mixed by horizontal and vertical advection. The analysis of the back trajectories allows us to gain qualitative information on the paths of the air masses associated with NPF events, and although they can be affected by an error estimated between 15 % and 30 % (Stohl, 1998; Draxler and Hess, 2004), for the purposes of this paper we considered negligible such inaccuracy. The main transport pathways to the study sites were identified by cluster analysis of back trajectories. Fig. 8 shows 6 centroids,

each representative of a group of trajectories, labelled according to the direction of the cluster, frequency of occurrence, and length. Short trajectories are indicative of slow-moving air masses while long trajectories are for fast flows; different lengths can have implications on a load of pollutants transported (associated) by air mass. As represented in Fig. 8, during the occurrence of NPF events the two stations were influenced by similar air masses, most of which were enclosed in the north-western quadrant. Air masses arriving at LMT and originating from the North-Northwester sector exhibited an occurrence rate of 38 % (17 % long and 20.5 % medium trajectories), followed by 62 % of air masses from the West-Northwest sector (9.8 % long, 19.6 % medium and 33 % short trajectories). At ECO, air masses originating from the North-Northwester sector showed a percentage of 20 % (medium trajectories), those from the West-Northwest sector an occurrence of 55 % (21.6 % long and 33.4 % short trajectories), while another important contribution, 25 % (short trajectory), was associated to Eastern sector. All the air masses flew over both the European continental areas highly anthropized and the marine environment before reaching the receptor points. It is interesting to note the lack of air masses associated with NPF events coming from the southern sector. These air masses, because of their pathway, are usually characterized by high levels of dust and humidity ~~collected during the crossing of the Mediterranean Sea. High levels of dust can~~ able to counter the NPF process because can suppress photochemical activity by scavenging reactive gases and condensable vapors (De Reus et al., 2000; Ndour et al., 2009).

We also focused on "common" NPF events considering only the air masses pathway related to these days detected during the study period. From 3-days back-trajectory analysis, emerged that the back-trajectories of common events exhibit similar characteristics in terms of origin and pathways to what already observed, but in addition, two different cases were detected, in the first the trajectory passes from ECO before reaching LMT, while in the other case, vice versa the air mass passes from LMT and then reaches ECO. Out of 50 common NPF events, 31 were in the first case and 19 in the second. Two representative examples of back-trajectories for each case are depicted in Fig. 9 and show that there is not a preferential path that can characterize them, because in both cases we find trajectories that come from both Eastern and Western Europe. These events occurred almost synchronously at the two sites, with a difference in starting time not greater than 30 minutes.

The factors that characterized the concomitant events of NPF (Table 4) are similar to those observed for the non-concomitant events, with values of $PM_{2.5}$, SO_2, CS and H_2SO_4 proxy in LMT lower than ECO, and similar meteorological conditions. The simultaneous observation of these events indicates that the formation of new particles has a wide horizontal extension and can be seen as a large-scale phenomenon. It is probable that the air masses already contain particles that have been formed by nucleation somewhere and then transported. Or during their travel, the air masses are enriched with gaseous precursors deriving from anthropogenic emissions and/or from biogenic production such as to foster (potentially) NPF processes, even in locations far from the sources.

~~It is interesting to note the lack of air masses associated with NPF events coming from the southern sector. These air masses, because of their pathway, are usually characterized by high levels of dust and humidity collected during the crossing of the Mediterranean Sea. High levels of dust can counter the NPF process because can suppress photochemical activity by scavenging reactive gases and condensable vapors (De Reus et al., 2000; Ndour et al., 2009).~~ These results emphasize the role that air masses have not only in terms of transport of precursors but also in synoptic atmospheric conditions to them associated.

In general, these results underline the importance of specific atmospheric conditions (temperature, solar radiation, RH, origin of air mass, pollutant concentrations) under which the NPF events have occurred and emphasize how the observed differences are associated with the levels of pollution found in them. The more frequent NPF events at the urban background compared to the coastal site can be ascribed to a greater abundance of condensable species, deriving from anthropogenic emissions, which favor the growth of particles increasing their chance of survival. Regarding the different seasonality of the events, while the trend at the urban site of ECO can be associated with the increased photochemical activity and the higher concentrations of different precursors during the warm months, the seasonality at the coastal site of LMT is more difficult to explain. Along with the lower availability of precursors, local conditions could play an additional role as well. These may include synoptic systems such as increased turbulence during warm months and the different atmospheric composition (related to the proximity to the sea and the effects of land-sea breezes) due to which the newly formed particles could be more effectively suppressed preventing further growth.

4 Conclusions

New particle formation events were studied and compared at two sites in southern Italy, ECO (Lecce) and LMT (Lamezia Terme) observatories, over a period of five years. The nucleation events occurred with a different frequency, 25 %, and 9 %, and seasonality, highest in spring-summer and autumn-winter at ECO and LMT, respectively.

Throughout the investigation period, 50 simultaneous NPF events (14 % of the cases in ECO and 40 % in LMT) were identified at both sites, many of which occurred in the colder months, indicating that the NPF process was affecting a large spatial extent. The NPF days were characterized by lower $PM_{2.5}$ concentrations (~60 % and 22 %) and higher SO_2 concentrations (~50 % and 20 %) compared to non-event days in LMT and ECO respectively, while the condensation sink seems not to be significantly different during events and non-event days. Marked differences in $PM_{2.5}$, SO_2, H_2SO_4 proxy, and CS levels were observed between the two sites, indicating the minor anthropogenic influence to which LMT is subjected. Common meteorological features were observed during NPF events that occurred in conditions of high pressure, low RH (~52 %), and moderate wind speed (3-4 m s^{-1}). The study of the back trajectories associated with the events also highlighted a common origin of the air masses, both of continental and marine origin, from the North-Northwest directions, suggesting that the chemical compounds involved in the NPF could have been transported by the air masses. Our founding let us assume that the lower levels of SO_2 and H_2SO_4 proxy (-60 % and -50% with respect to ECO) together with a different chemical composition of the aerosols and different local meteorology might be the reason for the lower frequency of events occurring in LMT, -60% with respect to ECO. The results presented in this paper are a contribution toward a better understanding of the complex NPF phenomenon in central Mediterranean area which will require further investigations and measurements of different precursors (such as ammonia, amines, VOCs) involved in the process that were not considered in this work.

Data Availability: Data is available upon request.

Author contributions: AD and DC conceptualized the study design. AD, DG and KW collaborated to data collection and post-processing. AD and DC prepared the draft. AD, DG, KW, IA, CC, AW, and DC, collaborated to interpretation of results, wrote, read, commented, and approved the final manuscript.

Competing interests: The authors declare no competing interests.

Acknowledgements: This work was supported by the project CIR01_00015 - PER-ACTRIS-IT "Potenziamento della componente italiana della Infrastruttura di Ricerca Aerosol, Clouds and Trace Gases Research Infrastructure - Rafforzamento del capitale umano" - Avviso MUR D.D. n. 2595 del 24.12.2019 Piano Stralcio "Ricerca e Innovazione 2015-2017".

References

Asmi, E., Kondratyev, V., Brus, D., Laurila, T., Lihavainen, H., Backman, J., Vakkari, V., Aurela, M., Hatakka, J., Viisanen, Y., Uttal, T., Ivakhov, V., and Makshtas, A.: Aerosol size distribution seasonal characteristics measured in Tiksi, Russian Arctic, Atmos. Chem. Phys., 16, 1271–1287, https://doi.org/10.5194/acp-16-1271-2016, 2016.

Asmi, E., Kivekäs, N., Kerminen, V.-M., Komppula, M., Hyvärinen, A.-P., Hatakka, J., Viisanen, Y., and Lihavainen, H.: Secondary new particle formation in Northern Finland Pallas site between the years 2000 and 2010, Atmos. Chem. Phys., 11, 12959–12972, doi:10.5194/acp-11-12959-2011, 2011.

Baalbaki, R., Pikridas, M., Jokinen, T., Laurila, T., Dada, L., Bezantakos, S., Ahonen, L., Neitola, K., Maisser, A., Bimenyimana, E., Christodoulou, A., Unga, F., Savvides, C., Lehtipalo, K., Kangasluoma, J., Biskos, G., Petäjä, T., Kerminen, V.-M., Sciare, J., and Kulmala, M.: Towards understanding the characteristics of new particle formation in the Eastern Mediterranean, Atmos. Chem. Phys., 21, 9223–9251, https://doi.org/10.5194/acp-21-9223-2021, 2021.

Backman, J., Rizzo, L. V., Hakala, J., Nieminen, T., Manninen, H. E., Morais, F., Aalto, P. P., Siivola, E., Carbone, S., Hillamo, R., Artaxo, P., Virkkula, A., Petäjä, T., and Kulmala, M.: On the diurnal cycle of urban aerosols, black carbon and the occurrence of new particle formation events in springtime São Paulo, Brazil, Atmos. Chem. Phys., 12, 11733–11751, https://doi.org/10.5194/acp-12-11733-2012, 2012.

Bianchi, F., Tr¨ostl, J., Junninen, H., Frege, C., Henne, S., Hoyle, C. R., Molteni, U., Herrmann, E., Adamov, A., Bukowiecki, N., Chen, X., Duplissy, J., Gysel, M., Hutterli, M., Kangasluoma, J., Kontkanen, J., Kürten, A., Manninen, H. E., Münch, S., and Baltensperger, U.: New particle formation in the free troposphere: A question of chemistry and timing, Science, 352, 1109–1112, DOI: 10.1126/science.aad5456, 2016.

Boulon, J., Sellegri, K., Hervo, M., and Laj, P.: Observations of nucleation of new particles in a volcanic plume, P. Natl. Acad. Sci. USA, 108, 12223–12226, doi:10.1073/pnas.1104923108, 2011.

Bousiotis, D., Pope, F. D., Beddows, D. C. S., Dall'Osto, M., Massling, A., Nøjgaard, J. K., Nordstrøm, C., Niemi, J. V., Portin, H., Petäjä, T., Perez, N., Alastuey, A., Querol, X., Kouvarakis, G., Mihalopoulos, N., Vratolis, S., Eleftheriadis, K., Wiedensohler, A., Weinhold, K., Merkel, M., Tuch, T., and Harrison, R. M.: A phenomenology of new particle formation (NPF) at 13 European sites, Atmos. Chem. Phys., 21, 11905–11925, https://doi.org/10.5194/acp-21-11905-2021, 2021.

Calidonna, C.R.; Avolio, E.; Gullì, D.; Ammoscato, I.; De Pino, M.; Donateo, A.; and Lo Feudo, T.: Five Years of Dust Episodes at the Southern Italy GAW Regional Coastal Mediterranean Observatory: Multisensor and Modelling Analysis, Atmos., 11, 456, ; https://doi.org/10.3390/atmos11050456, 2020.

Casquero-Vera, J.A.; Lyamani, H., Dada, L., Hakala, S., Paasonen, P., Román, R. Fraile, R., Petäjä, T., Olmo-Reyes, F.J., Alados-Arboledas, L.: New particle formation at urban and high-altitude remote sites in the South-Eastern Iberian Peninsula, Atmos. Chem. Phys., 20 (22), 14253-14271, 10.5194/acp-20-14253, 2020.

Casquero-Vera, J.A., Lyamani, H., Titos, G., Minguillón, M.C., Dada, L., Alastuey, A., Querol, X., Petäjä, T., Olmo, F.J., Alados-Arboledas, L.: Quantifying traffic, biomass burning and secondary source contributions to atmospheric particle number concentrations at urban and suburban sites, Science of The Total Environment, 145282, https://doi.org/10.1016/j.scitotenv.2021.145282, 2021.

Conte, M., Merico, E., Cesari, D., Dinoi, A., Grasso, F.M., Donateo, A., Guascito, M.R., and Contini, D.: Long-term characterisation of African dust advection in south-eastern Italy: Influence on fine and coarse particle concentrations, size distributions, and carbon content, Atmos. Res., 233, 104690, https://doi.org/10.1016/j.atmosres.2019.104690, 2020.

Cristofanelli, P., Busetto, M., Calzolari, F., Ammoscato, I., Gullì, D., Dinoi, A., Calidonna, C.R., Contini, D., Sferlazzo, D., Di Iorio, T., Piacentino, S., Marinoni, A., Maione, M., and Bonasoni, P.: Investigation of reactive gases and methane variability in the coastal boundary layer of the central Mediterranean basin, Elem. Sci. Anthr., 5, 12, https://doi.org/10.1525/elementa.216, 2017.

Cusack, M., Pérez, N., Pey, J., Alastuey, A., and Querol, X.: Source apportionment of fine PM and sub-micron particle number concentrations at a regional background site in the western Mediterranean: a 2.5-year study, Atmos. Chem. Phys. 13, 5173–5187, https://doi.org/10.5194/acp-13-5173-2013, 2013.

Dai, L., Wang, H. L., Zhou, L. Y., An, J. L., Tang, L. L., Lu, C. S., Yan, W. L., Liu, R. 466 Y., Kong, S. F., Chen, M. D., Lee, S. H., and Yu, H.: Regional and local new particle formation events observed in the Yangtze River Delta region, China, J. Geophys. Res. Atmos. 122 2389–402, https://doi.org/10.1002/2016JD026030, 2017.

Dal Maso, M., Kulmala, M., Riipinen, I., Wagner, R., Hussein, T., Aalto, P. P., and Lehtinen, K. E. J.: Formation and growth of fresh atmospheric aerosols: eight years of aerosol size distribution data from SMEAR II, Hyytiala, Finland, Boreal, Environ Res, 10, 323-336, 2005.

Dall'Osto, M., Querol, X., Alastuey, A., O'Dowd, C., Harrison, R. M., Wenger, J., and Gómez-Moreno, F. J.: On the spatial distribution and evolution of ultrafine particles in Barcelona, Atmos. Chem. Phys., 13, 741–759, https://doi.org/10.5194/acp-13-741-2013, 2013.

Debevec, C., Sauvage, S., Gros, V., Sellegri, K., Sciare, J., Pikridas, M., Stavroulas, I., Leonardis, T., Gaudion, V., Depelchin, L., Fronval, I., Sarda-Esteve, R., Baisnée, D., Bonsang, B., Savvides, C., Vrekoussis, M., and Locoge, N.: Driving parameters of biogenic volatile organic compounds and consequences on new particle formation observed at an eastern Mediterranean background site, Atmos. Chem. Phys., 18, 14297–14325, https://doi.org/10.5194/acp-18-14297-2018, 2018.

De Reus, M., Dentener, F., Thomas, A., Borrmann, S., Strom, J., and Lelieveld, J.: Airborne observations of dust aerosol over the North Atlantic Ocean during ACE-2: indications for heterogeneous ozone destruction, J. Geophys. Res., 105, 15 263–15 275, https://doi.org/10.1029/2000JD900164, 2000.

Dinoi, A., Conte, M., Grasso, F.M., and Contini, D.: Long-term characterization of submicron atmospheric particles in an urban background site in Southern Italy, Atmos., 11, 334, https://doi.org/10.3390/atmos11040334, 2020.

Dinoi, A., Weinhold, K., Wiedensohler, A., Contini, D.: Study of new particle formation events in southern Italy, Atmos. Env., 244, 117920, https://doi.org/10.1016/j.atmosenv.2020.117920, 2021a.

Dinoi, A., Gulli, D., Ammoscato, I., Calidonna, C.R., and Contini, D.: Impact of the coronavirus pandemic lockdown on atmospheric nanoparticle concentrations in two sites of Southern Italy, Atmos., 12, 352, https://doi.org/10.3390/atmos12030352, 2021b.

Donateo, A., Lo Feudo, T., Marinoni, A., Dinoi, A., Avolio, E., Merico, E., Calidonna, C.R., Contini, D., and Bonasoni, P.: Characterization of in situ aerosol optical properties at three observatories in the Central Mediterranean, Atmos., 9, 369, https://doi.org/10.3390/atmos9100369, 2018.

Draxler, R., and Hess, G. D.: An overview of the HYSPLIT 4 modeling system for trajectories, dispersion and deposition, Australian Meteorological Magazine, 47, 295–308, 1998.

Draxler R. R. and Hess, G. D.: Description of the HYSPLIT 4 Modeling System, NOAA Technical Memorandum ERL ARL-224, 2004.

Franco, M. A., Ditas, F., Kremper, L. A., Machado, L. A. T., Andreae, M. O., Araújo, A., Barbosa, H. M. J., de Brito, J. F., Carbone, S., Holanda, B. A., Morais, F. G., Nascimento, J. P., Pöhlker, M. L., Rizzo, L. V., Sá, M., Saturno, J., Walter, D., Wolff, S., Pöschl, U., Artaxo, P., and Pöhlker, C.: Occurrence and growth of sub-50 nm aerosol particles in the Amazonian boundary layer, Atmos. Chem. Phys., 22, 3469–3492, https://doi.org/10.5194/acp-22-3469-2022, 2022.

Fuchs, N. A. and Sutugin, A. G.: Highly dispersed aerosols, in: Topics in Current Aerosol Research, edited by: Hidy, G. M. and Brock, J. R., p. 1, Pergamon, New York, 1971.

Hussein, T., Molgaard, B., Hannuniemi, H., Martikainen, J., Järvi, L., Wegner, T., Ripamonti, G., Weber, S., Vesala, T., and Hämeri, K.: Fingerprints of the urban particle number size distribution in Helsinki, Finland: Local vs. regional characteristics, Boreal Env. Res., 19, 1–20, 2014.

Hussein, T., Atashi, N., Sogacheva, L.; Hakala, S., Dada, L., Petaja, T., Kulmala, M.: Characterization of Urban New Particle Formation in Amman—Jordan, Atmos., 11(1), 79. https://doi.org/10.3390/atmos11010079, 2020.

Jensen, D.D.; Price, T.A.; Nadeau, D.F.; Kingston, J.; and Pardyjak, E.R.: Coastal Wind and Turbulence Observations during the Morning and Evening Transitions over Tropical Terrain, J. Appl. Meteorol. Climatol., 56, 3167–3185, https://doi.org/10.1175/JAMC-D-17-0077.1, 2017.

Jokinen, T., Lehtipalo, K., Thakur, R. C., Ylivinkka, I., Neitola, K., Sarnela, N., Laitinen, T., Kulmala, M., Petäjä, T., and Sipilä, M.: Measurement report: Long-term measurements of aerosol precursor concentrations in the Finnish subarctic boreal forest, Atmos. Chem. Phys., 22, 2237–2254, https://doi.org/10.5194/acp-22-2237-2022, 2022.

Kalivitis, N., Kerminen, V.-M., Kouvarakis, G., Stavroulas, I., Tzitzikalaki, E., Kalkavouras, P., Daskalakis, N., Myriokefalitakis, S., Bougiatioti, A., Manninen, H. E., Roldin, P., Petäjä, T., Boy, M., Kulmala, M., Kanakidou, M., and Mihalopoulos, N.: Formation and growth of atmospheric nanoparticles in the eastern Mediterranean: results from long-term measurements and process simulations, Atmos. Chem. Phys., 19, 2671–2686, https://doi.org/10.5194/acp-19-2671-2019, 2019.

Kalkavouras, P., Bougiatioti, A., Grivas, G., Stavroulas, I., Kalivitis, N., Liakakou, E., Gerasopoulos, E., Pilinis, C., and Mihalopoulos, N.: On the regional aspects of new particle formation in the Eastern Mediterranean: A comparative study between a background and an urban site based on long term observations, Atmos. Res., 239, 104911, https://doi.org/10.1016/j.atmosres.2020.104911, 2020.

Kerminen, V.-M., Chen, X., Vakkari, V., Pet¨aj¨a, T., Kulmala, M., and Bianchi, F.: Atmospheric new particle formation and growth: Review of field observations. Env. Res. Letters, 13, 103003, https://doi.org/10.1088/1748-9326/aadf3c, 2018.

Kopanakis, I., Chatoutsidou, S. E., Torseth, K., Glytsos, T., and Lazaridis, M.: Particle number size distribution in the eastern Mediterranean: Formation and growth rates of ultrafine airborne atmospheric particles, Atmos. Environ., 77, 790–802, doi:10.1016/j.atmosenv.2013.05.066, 2013.

Kulmala, M., Petäjä, T., Nieminen, T., Sipilä, M., Manninen, H.E., Lehtipalo, K., Dal Maso, M., Aalto, P.P., Junninen, H., Paasonen, P., Riipinen, I., Lehtinen, K.E.J., Laaksonen, A., and Kerminen, V.-M.: Measurement of the nucleation of atmospheric aerosol particles. Nat. Protoc. 7, 1651–1667, http://dx.doi.org/10.1038/nprot.2012.091, 2012.

Lehtinen, K. E. J. and Kulmala, M.: A model for particle formation and growth in the atmosphere with molecular resolution in size, Atmos. Chem. Phys., 3, 251–257, 2003.

Merikanto, J., Spracklen, D. V., Mann, G. W., Pickering, S. J., and Carslaw, K. S.: Impact of nucleation on global CCN, Atmos. Chem. Phys., 9, 8601–8616, https://doi.org/10.5194/acp-9-8601-2009, 2009.

Minguillón, M. C., Ripoll, A., Pérez, N., Prévôt, A. S. H., Canonaco, F., Querol, X., and Alastuey, A.: Chemical characterization of submicron regional background aerosols in the western Mediterranean using an Aerosol Chemical Speciation Monitor, Atmos. Chem. Phys., 15, 6379–6391, https://doi.org/10.5194/acp-15-6379-2015, 2015.

Mirme, S., Mirme, A., Minikin, A., Petzold, A., Hõrrak, U., Kerminen, V.-M., and Kulmala, M.: Atmospheric sub-3 nm particles at high altitudes, Atmos. Chem. Phys., 10, 437–451, https://doi.org/10.5194/acp-10-437-2010, 2010.

Ndour, M., Conchon, P., D'Anna, B., Ka, O., and George, C.: Photochemistry of mineral dust surface as a potential atmospheric renoxification process, Geophys. Res. Lett., 36, 5, https://doi.org/10.1029/2008GL036662, 2009.

Németh, Z. and Salma, I.: Spatial extension of nucleating air masses in the Carpathian Basin, Atmos. Chem. Phys., 14, 8841–8848, https://doi.org/10.5194/acp-14-8841-2014, 2014.

Nemeth, Z., Rosat, B., Zikova, N., Salma, I., Bozo, L., de Espana, C. D., Schwarz, J., Zdimal, V. and Wonaschügtz, A.: Comparison of atmospheric new particle formation events in three Central European cities, Atmos. Environ., 178, 191–7, https://doi.org/10.1016/j.atmosenv.2018.01.035, 2018.

Nieminen, T., Kerminen, V.-M., Petäjä, T., Aalto, P. P., Arshinov, M., Asmi, E., Baltensperger, U., Beddows, D. C. S., Beukes, J. P., Collins, D., Ding, A., Harrison, R. M., Henzing, B., Hooda, R., Hu, M., Hõrrak, U., Kivekäs, N., Komsaare, K., Krejci, R., Kristensson, A., Laakso, L., Laaksonen, A., Leaitch, W. R., Lihavainen, H., Mihalopoulos, N., Németh, Z., Nie, W., O'Dowd, C., Salma, I., Sellegri, K., Svenningsson, B., Swietlicki, E., Tunved, P., Ulevicius, V., Vakkari, V., Vana, M., Wiedensohler, A., Wu, Z., Virtanen, A., and Kulmala, M.: Global analysis of continental boundary layer new particle formation based on longterm measurements, Atmos. Chem. Phys., 18, 14737–14756, https://doi.org/10.5194/acp-18-14737-2018, 2018.

Petäjä, T., Mauldin III, R. L., Kosciuch, E., McGrath, J., Nieminen, T., Paasonen, P., Boy, M., Adamov, A., Kotiaho, T., and Kulmala, M.: Sulfuric acid and OH concentrations in a boreal forest site, Atmos. Chem. Phys., 9, 7435–7448, https://doi.org/10.5194/acp9-7435-2009, 2009.

Pikridas, M., Vrekoussis, M., Sciare, J., Kleanthous, S., Vasiliadou, E., Kizas, C., Savvides, C., and Mihalopoulos, N.: Spatial and temporal (short and long-term) variability of submicron, fine and sub-10 μm particulate matter (PM1, PM2.5, PM10) in Cyprus, Atmos. Env., 191, 79-93, https://doi.org/10.1016/j.atmosenv.2018.07.048, 2018.

Putaud, J.-P., Van Dingenen, R., Alastuey, A., Bauer, H., Birmili, W., Cyrys, J., Flentje, H., Fuzzi, S., Gehrig, R., Hansson, H.C., Harrison, R.M., Herrmann, H., Hitzenberger, R., Hüglin, C., Jones, A.M., Kasper-Giebl, A., Kiss, G., Kousa, A., Kuhlbusch, T.A.J., Löschau, G., Maenhaut, W., Molnar, A., Moreno, T., Pekkanen, J., Perrino, C., Pitz, M., Puxbaum, H., Querol, X., Rodriguez, S., Salma, I., Schwarz, J., Smolik, J., Schneider, J., Spindler, G., ten Brink, H., Tursic, J., Viana, M., Wiedensohler, A., and Raes, F.: A European aerosol phenomenology – 3: Physical and chemical characteristics of particulate matter from 60 rural, urban, and kerbside sites across Europe, Atmos. Env., 44, 1308-1320, https://doi.org/10.1016/j.atmosenv.2009.12.011, 2010.

Querol, X., Gangoiti, G., Mantilla, E., Alastuey, A., Minguillón, M. C., Amato, F., Reche, C., Viana, M., Moreno, T., Karanasiou, A., Rivas, I., Pérez, N., Ripoll, A., Brines, M., Ealo, M., Pandolfi, M., Lee, H.-K., Eun, H.-R., Park, Y.-H., Escudero, M., Beddows, D., Harrison, R.M., Bertrand, A., Marchand, N., Lyasota, A., Codina, B., Olid, M., Udina, M., Jiménez-Esteve, B., Soler, M.R., Alonso, L., Millán, M., and Ahn, K.-H.: Phenomenology of high-ozone episodes in NE Spain, Atmos. Chem. Phys. 17, 2817-2838, https://doi.org/10.5194/acp-17-2817-2017, 2017.

Rose, C., Sellegri, K., Velarde, F., Moreno, I., Ramonet, M., Weinhold, K., Krejci, R., Ginot, P., Andrade, M., Wiedensohler, A., and Laj, P.: Frequent nucleation events at the high altitude station of Chacaltaya (5240 m a.s.l.), Bolivia, Atmos. Env., 102, 18-29, https://doi.org/10.1016/j.atmosenv.2014.11.015, 2015.

Saha, P.K., Robinson, E.S., Shah, R.U., Zimmerman, N., Apte, J.S., Robinson, A.L., and Presto, A.A.: Reduced ultrafine particle concentration in urban air: changes in nucleation and anthropogenic emissions, Environ. Sci. Technol., 52 (12), 6798-6806, https://doi.org/10.1021/acs.est.8b00910, 2018.

Salma, I., Németh, Z., Kerminen, V.-M., Aalto, P., Nieminen, T., Weidinger, T., Molnár, Á., Imre, K., and Kulmala, M., Regional effect on urban atmospheric nucleation, Atmos. Chem. Phys. 16, 8715–8728, 2016.

Salma, I., Varga, V., and Németh, Z.: Quantification of an atmospheric nucleation and growth process as a single source of aerosol particles in a city, Atmos. Chem. Phys., 17, 15007– 15017, https://doi.org/10.5194/acp-17-15007-2017, 2017.

Salma, I., and Németh, Z.: Dynamic and timing properties of new aerosol particle formation and consecutive growth events. Atmos. Chem. Phys., 19, 5835–5852, https://doi.org/10.5194/acp-19-5835-2019, 2019.

Sartelet, K., Kim, Y., Couvidat, F., Merkel, M., Petäjä, T., Sciare, J., and Wiedensohler, A.: Influence of emission size distribution and nucleation on number concentrations over Greater Paris, Atmos. Chem. Phys., 22, 8579–8596, https://doi.org/10.5194/acp-22-8579, 2022.

Schroder, F., and J. Strom, Aircraft measurements of sub micrometer aerosol particles (>7 nm) in the mid-latitude free troposphere and troposphere region, Atmos. Res., 44, 333-356, https://doi.org/10.1016/S0169-8095(96)00034-8,1997.

Sipilä, M., Berndt, T., Petäjä, T., Brus, D., Vanhanen, J., Stratmann, F., Patokoski, J., Mauldin, R. L., Hyvärinen, A.- P., Lihavainen, H., and Kulmala, M.: The Role of Sulfuric Acid in Atmospheric Nucleation, Science, 327, 1243–1246, https://doi.org/10.1126/science.1180315, 2010.

Stohl, A., Hittenberger, M., and Wotawa, G.: Validation of the Lagrangian particle dispersion model FLEXPART against large scale tracer experiment data, Atmos. Environ., 32, 4245–4264, https://doi.org/10.1016/S1352-2310(98)00184-8, 1998.

Thén, W.; Salma, I.: Particle Number Concentration: A Case Study for Air Quality Monitoring. Atmosphere, 13, 570, https://doi.org/10.3390/atmos13040570, 2022.

Wehner, B., Werner, F., Ditas, F., Shaw, R. A., Kulmala, M., and Siebert, H.: Observations of new particle formation in enhanced UV irradiance zones near cumulus clouds, Atmos. Chem. Phys., 15, 11701–11711, https://doi.org/10.5194/acp-15-11701-2015, 2015.

Wiedensohler, A., Birmili, W., Nowak, A., Sonntag, A., Weinhold, K., Merkel, M., Wehner, B., Tuch, T., Pfeifer, S., Fiebig, M., Fjäraa, A. M., Asmi, E., Sellegri, K., Depuy, R., Venzac, H., Villani, P., Laj, P., Aalto, P., Ogren, J. A., Swietlicki, E., Williams, P., Roldin, P., Quincey, P., Hüglin, C., Fierz-Schmidhauser, R., Gysel, M., Weingartner, E., Riccobono, F., Santos, S., Grüning, C., Faloon, K., Beddows, D., Harrison, R., Monahan, C., Jennings, S. G., O'Dowd, C. D., Marinoni, A., Horn, H.-G., Keck, L., Jiang, J., Scheckman, J., McMurry, P. H., Deng, Z., Zhao, C. S., Moerman, M., Henzing, B., de Leeuw, G., Löschau, G., and Bastian, S.: Mobility particle size spectrometers: harmonization of technical standards and data structure to facilitate high quality long-term observations of atmospheric particle number size distributions, Atmos. Meas. Tech., 5, 657–685, https://doi.org/10.5194/amt-5-657-2012, 2012.

Wonaschütz, A., Demattio, A., Wagner, R., Burkart, J., Zíková, N., Vodička, P., Ludwig, W., Steiner, G., Schwarz, J., and Hitzenberger, R.: Seasonality of new particle formation in Vienna, Austria - influence of air mass origin and aerosol chemical composition. Atmos. Environ. 118, 118–126, https://doi.org/10.1016/j.atmosenv.2015.07.035, 2015.

Wu, H., Li, Z., Li, H., Luo, K., Wang, Y., Yan, P., Hu, F., Zhang, F., Sun, Y., Shang, D., Liang, C., Zhang, D., Wei, J., Wu, T., Jin, X., Fan, X., Cribb, M., Fischer, M. L., Kulmala, M., and Petäjä, T.: The impact of the atmospheric turbulence-development tendency on new particle formation: a common finding on three continents, Nat. Sci. Rev., 8, 3, nwaa157, https://doi.org/10.1093/nsr/nwaa157, 2021.

Yadav, S. K., Kompalli, S. K., Gurjar, B. R., and Mishra, R. K.: Aerosol number concentrations and new particle formation events over a polluted megacity during the COVID-19 lockdown, Atmos. Environ., 259, 118526, https://doi.org/10.1016/j.atmosenv.2021.118526, 2021.

Yu, F., Luo, G., Nair, A. A., Schwab, J. J., Sherman, J. P., and Zhang, Y.: Wintertime new particle formation and its contribution to cloud condensation nuclei in the Northeastern United States, Atmos. Chem. Phys., 20, 2591–2601, https://doi.org/10.5194/acp-20-2591-2020, 2020.

Zhang, Q. J., Beekmann, M., Freney, E., Sellegri, K., Pichon, J. M., Schwarzenboeck, A., Colomb, A., Bourrianne, T., Michoud, V., and Borbon, A.: Formation of secondary organic aerosol in the Paris pollution plume and its impact on surrounding regions, Atmos. Chem. Phys., 15, 13973–13992, https://doi.org/10.5194/acp-15-13973-2015, 2015.

Zhu, Y.J., Sabaliauskas, K., Liu, X.H., Meng, H., Gao, H.W., Jeong, C.-H., Evans, G., and Yao, X.H.: Comparative analysis of new particle formation events in less and severely polluted urban atmosphere, Atmos. Env., 98, 655-664, https://doi.org/10.1016/j.atmosenv.2014.09.043, 2014.

Figures

Figure 1: Map of the exanimated area with the locations of the two environmental-climate observatories, ECO and LMZ. The map was retrieved from Google (Map data © 2022).

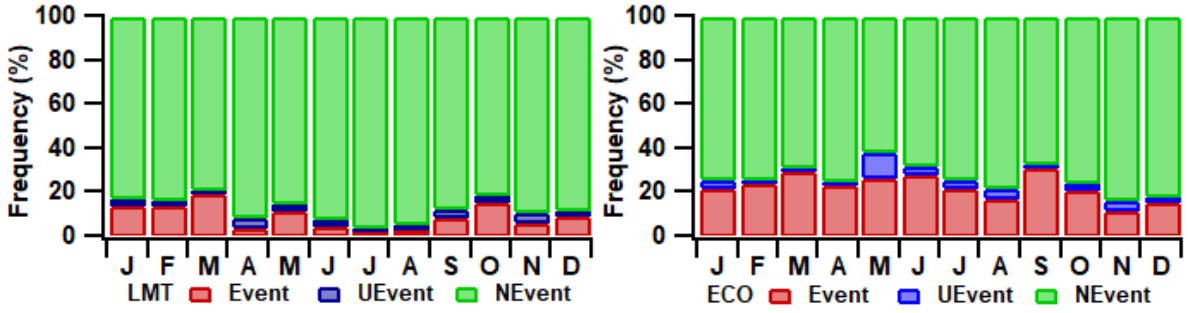

Fig. 2. Monthly percentage of occurrence of Events (red bars), Undefined events (blue bars), and Non-Events (green bars) related to available measurement days at LMT and ECO.

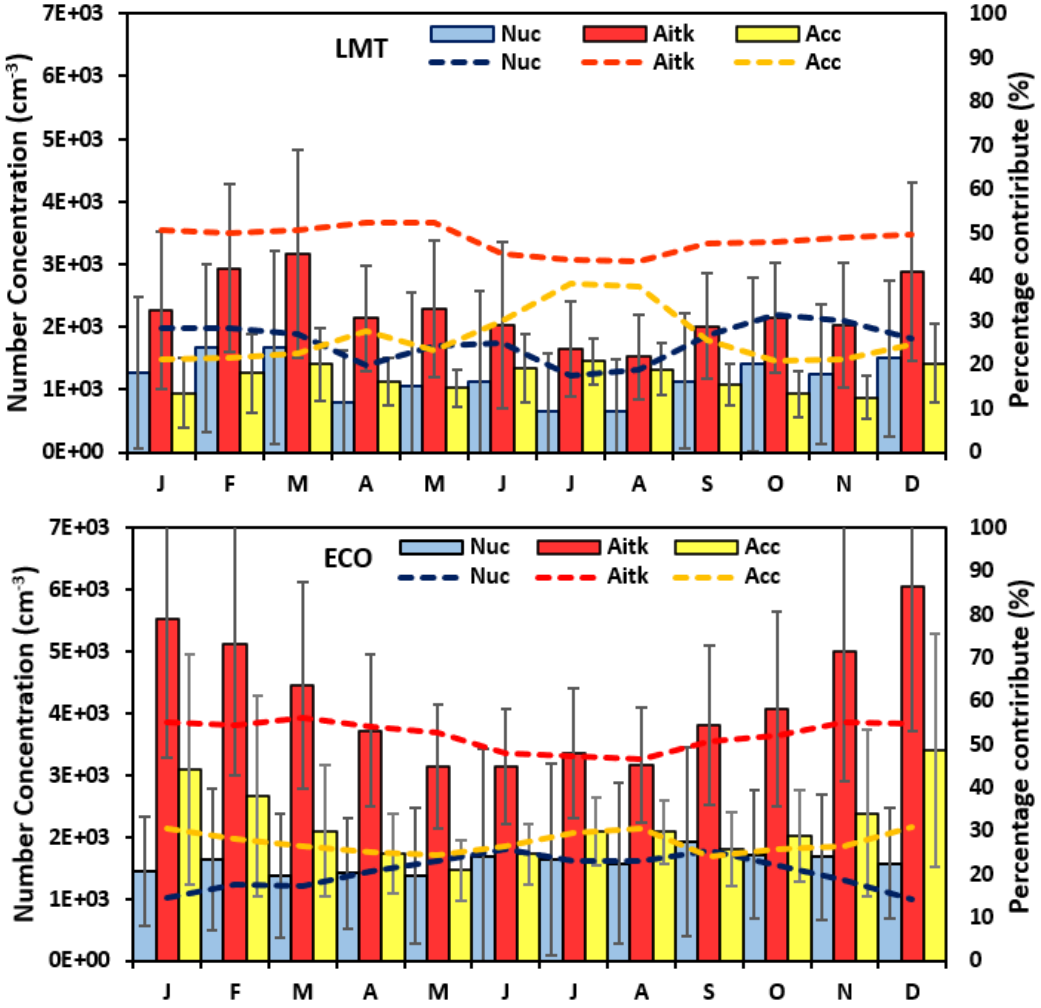

Fig. 3. Average monthly variation (bars) of the nucleation, Aitken, and accumulation mode particle number concentration over the whole period of study at LMT and ECO. The dashed lines represent the monthly percentage contribution of each particle fraction to total particle number concentration.

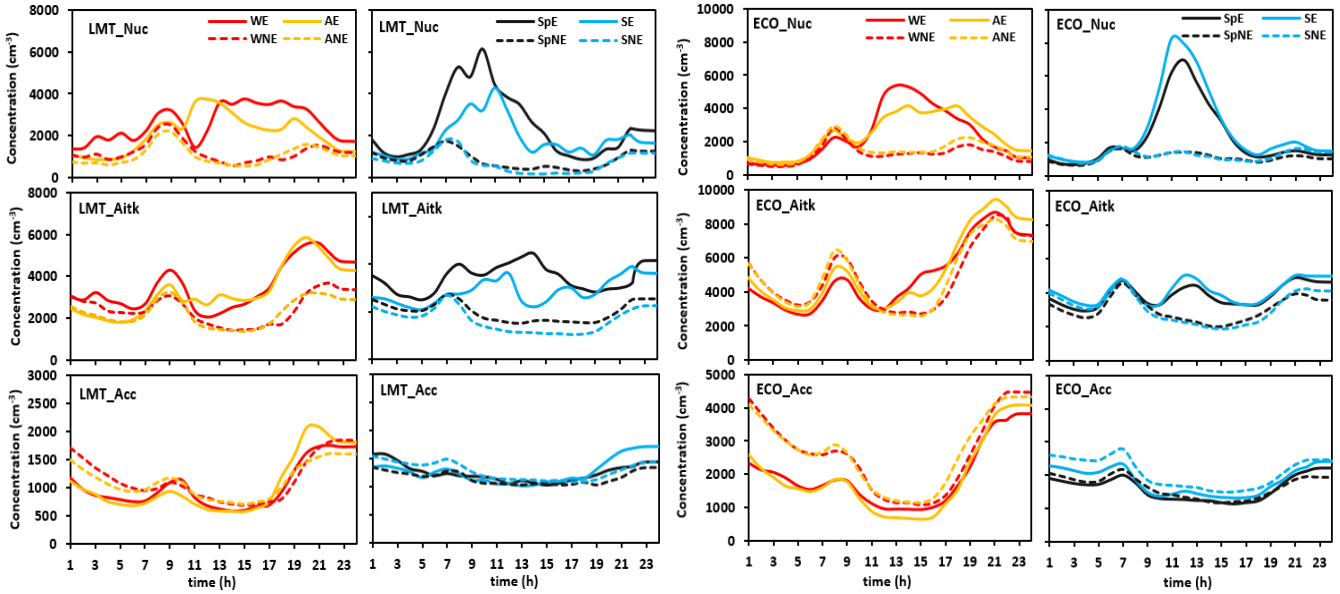

Fig. 4. Average diurnal variation in nucleation, Aitken, and accumulation mode particle number concentration (from top to bottom) over the whole period of study at LMT and ECO. Solid lines are for NPF events days (E) and dashed lines for non-events days of (NE), red for winter, grey for spring, blue for summer, and yellow for autumn.

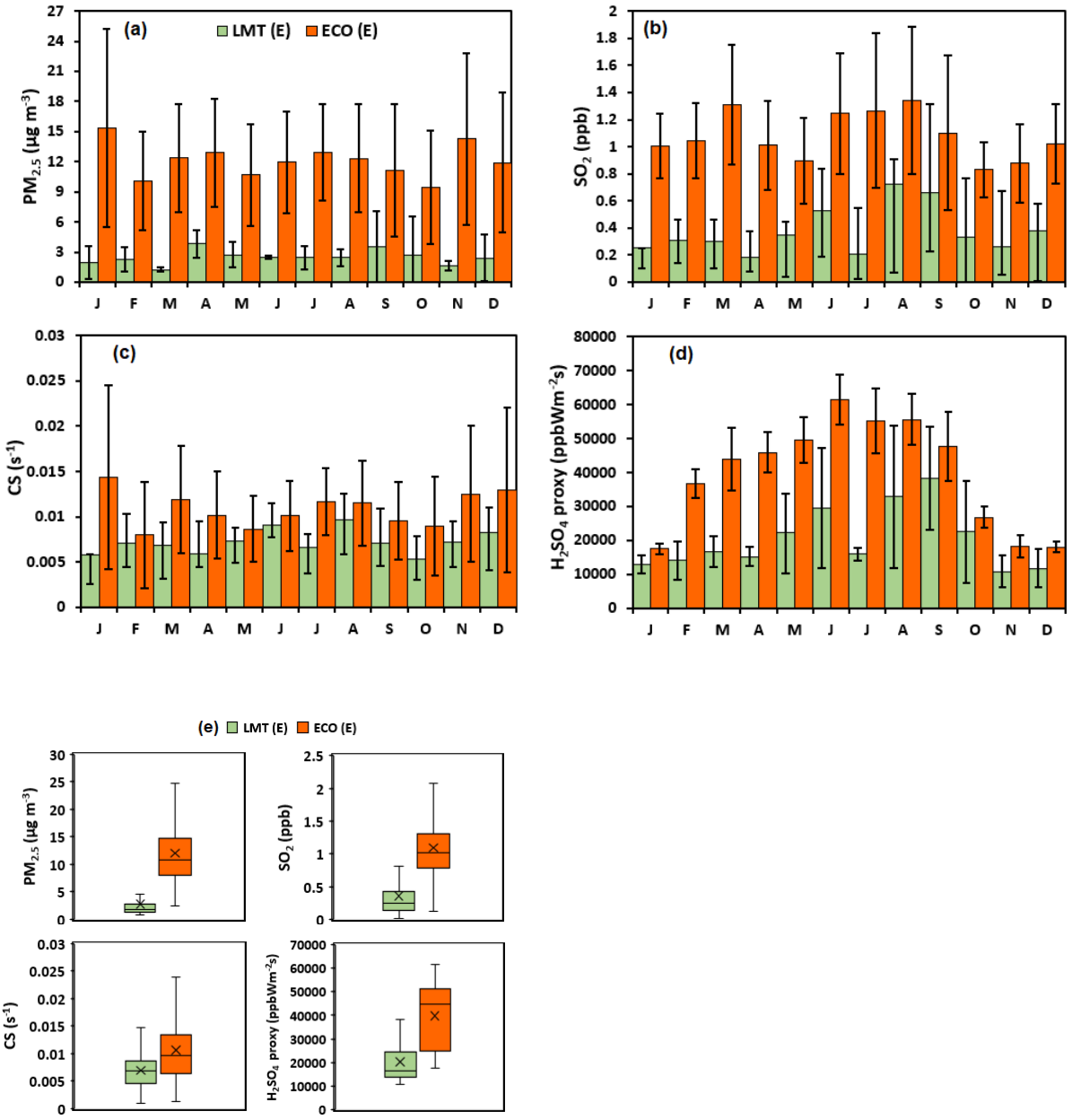

Fig. 5. Monthly means of (a) $PM_{2.5}$, (b) SO_2, (c) CS and (d) H_2SO_4 proxy related to event days for LMT (green) and ECO (red). The bars indicate the standard deviation. (e) Box plot of $PM_{2.5}$, SO_2, CS and H_2SO_4 proxy associated with event days for LMT (green) and ECO (red). The box shows the quartiles, the median (the line inside the box), the mean (the star), and 90 th and 10 th percentiles (the whiskers).

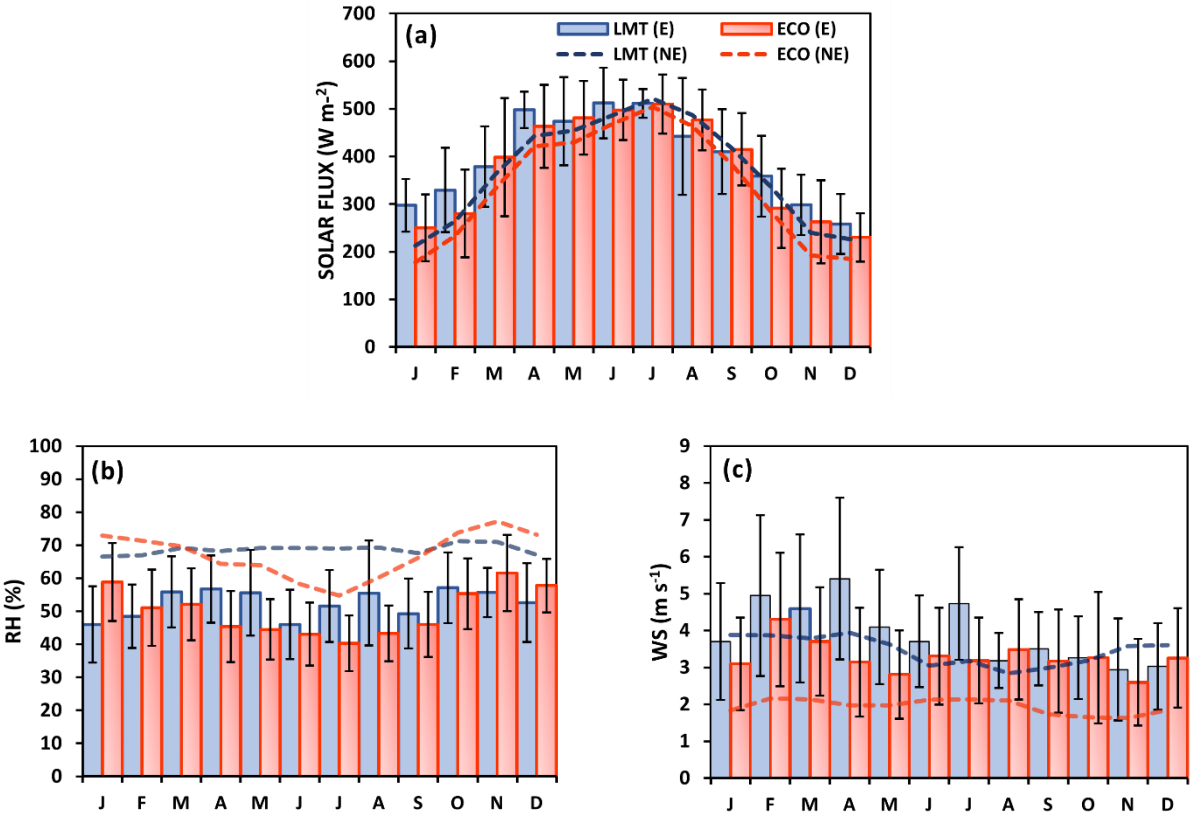

685 **Fig. 6. Monthly means of (a) solar flux, (b) relative humidity, and (c) wind speed related to event days (columns) and non-event days (dashed lines) for LMT (blue) and ECO (red). The bars indicate the standard deviation.**

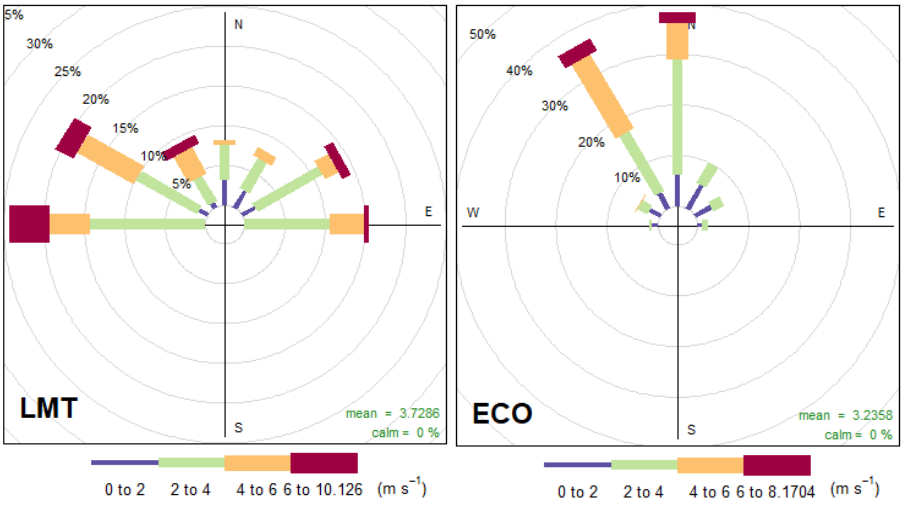

690

Figure 7. Wind roses related to event days for LMT and ECO observatories.

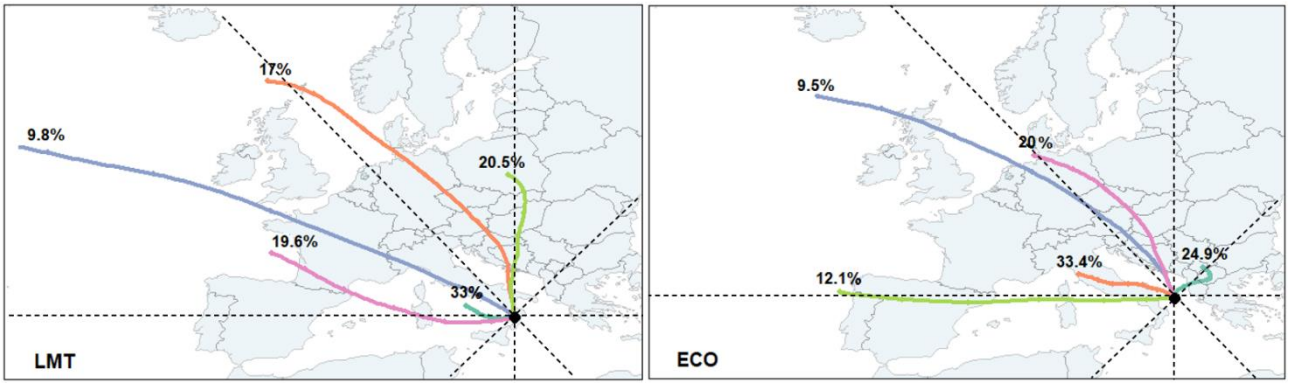

Fig. 8. Cluster centroids retrieved from the 3-day analytical back trajectories reaching ECO and LMT at 500m above sea levels. The maps were plotted using Hysplit integrated with the Openair package.

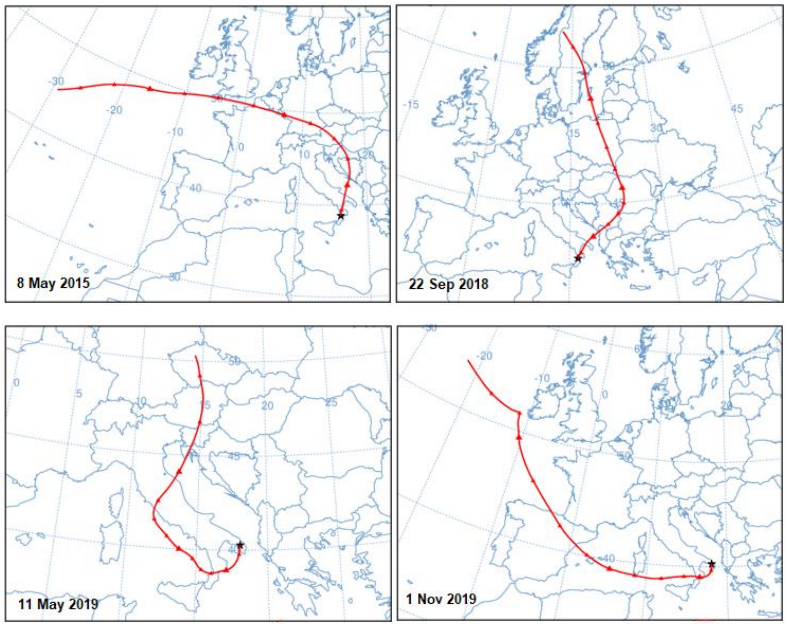

Fig. 9. 72 h back-trajectories arriving at LMT (up) and ECO (down) during four simultaneous new-particle formation events. The maps were retrieved from NOAA Hysplit Model.

Tables

Table 1. Number of available days (N) and relative frequencies (f %) of each class, NPF events, non-events, and undefined events detected in ECO and LMT observatories.

	LMT (Total=1440)		ECO (Total=1423)	
Day Classification	Number	Frequency (%)	Number	Frequency (%)
NPF events	124	9	352	25
Non-events	1272	88	1019	71
Undefined events	44	3	52	4

Table 2. Arithmetic means ± 1 standard deviation and medians (25th–75th) percentiles of total, accumulation, Aitken, and nucleation PNC (cm^{-3}) for both sites.

	Nnuc ($10^3 cm^{-3}$)	Naitk ($10^3 cm^{-3}$)	Nacc ($10^3 cm^{-3}$)	Ntot ($10^3 cm^{-3}$)
LMT	1.1±1.0	2.2±1.1	1.2±0.6	4.4±2.2
	0.7 (0.3-1.5)	1.9 (1.4-2.7)	1.0 (0.7-1.0)	4.0 (2.8-5.6)
ECO	1.6 ±1.0	4.1±1.8	2.1±1.4	7.8±3.4
	1.3 (0.9-1.9)	3.7 (2.8-4.8)	1.8 (1.2-2.6)	7.1 (5.5-9.3)

Table 3. Arithmetic means ± 1 standard deviation of nucleation, Aitken and accumulation PNC (cm^{-3}) related to event days (E) and non-event days (NE) for each season (winter W, spring Sp, summer S, and autumn A) and for both sites.

	LMT			ECO		
	Nnuc ($10^3 cm^{-3}$)	Naitk ($10^3 cm^{-3}$)	Nacc ($10^3 cm^{-3}$)	Nuc ($10^3 cm^{-3}$)	Naitk ($10^3 cm^{-3}$)	Nacc ($10^3 cm^{-3}$)
W (E)	2.5±0.8	3.5±1.1	1.0±0.4	2.3±1.6	4.9±1.9	1.9±0.9
W (NE)	1.2±0.5	2.4±0.7	1.1±0.4	1.2±0.6	4.8±1.8	2.6±1.2
Sp (E)	2.4±1.5	3.4±0.6	1.2±0.2	2.2±1.8	3.8±0.6	1.6±0.3
Sp (NE)	0.8±0.4	2.0±0.4	1.2±0.2	1.1±0.3	3.0±0.7	1.6±0.3
S (E)	1.8±0.9	2.9±0.5	1.3±0.2	2.7±2.2	4.1±0.7	1.8±0.4
S (NE)	0.7±0.4	1.6±0.5	1.3±0.2	1.2±0.3	3.1±0.9	2.1±0.4
A (E)	2.0±0.9	3.3±1.2	1.0±0.5	2.4±1.2	5.2±2.2	1.9±1.1
A (NE)	1.1±0.4	2.3±0.6	1.1±0.3	1.5±0.6	4.9±1.9	2.7±1.1

Table 4. Arithmetic means ± 1 standard deviation and medians (25 th–75 th) percentiles of different parameters, $PM_{2.5}$, SO_2, CS, H_2SO_4, GR, RH, WS and SF for both sites.

730

	$PM_{2.5}$ ($\mu g\ m^{-3}$)	SO_2 (ppb)	CS $x10^2$ (s^{-1})	H_2SO_4 $x10^3$ ($ppbWm^{-2}s^{-1}$)	GR ($nm\ h^{-1}$)	RH (%)	WS ($m\ s^{-1}$)	SF ($W\ m^{-2}$)
LMT	3.1±2.6	0.3±0.3	0.6±3.0	21±19	6.7±2.6	48±10	4.2±1.4	394±110
	2.0 (1.3-4.2)	0.2 (0.2-0.4)	0.6 (0.4-0.8)	15 (10-23)	6.2 (5.0-8.2)	50 (40-56)	3.9 (3.0-5.0)	360 (313-496)
ECO	8.9±4.8	0.9±0.3	0.9±0.6	38±23	6.6±2.0	49±12	3.8±1.7	365±133
	8.0 (5.1-11.0)	0.9 (0.8-1.0)	0.8 (0.8-1.0)	39 (26-62)	6.6 (5.0-7.6)	48 (41-56)	3.5 (2.2-4.9)	350 (340-470)